Mesophase Transitions, Surface Functionalization, and Growth Mechanism of Semiconducting 6PTTP6 Films from Solution†

Howard E. Katz,*,‡ Theo Siegrist,*,‡ Michael Lefenfeld,‡ Padma Gopalan,‡ Melissa Mushrush,‡ Ben Ocko*,§ Oleg Gang,§ and Najeh Jisrawl§

Bell Laboratories, Lucent Technologies, 600 Mountain Avenue, Murray Hill, New Jersey 07974, and Brookhaven National Laboratories, P.O. Box 5000, Upton, New York 11973-5000

Received: October 10, 2003

The grain structure is compared for films of the organic semiconductor 6PTTP6 prepared in the open air and in a closed, static atmosphere saturated with xylene vapor. The effect of surface functional groups affixed to the dielectric substrate on the grain appearance and film mobility is probed, to determine optimal fabrication conditions for films with usable mobility, high on/off ratio, and good uniformity. A single-crystal device, also obtained from solution deposition under a particular set of conditions, is characterized and displays an expected higher mobility, >0.1 cm^2/Vs. Mesophases are identified in the presence and absence of the xylene and tentatively identified through polarized optical microscopy (POM). Finally, a preliminary observation of the film evolution using an in situ X-ray diffraction (XRD) technique is reported, and lattice spacings are assigned.

I. Introduction

Organic field-effect transistor (FET) semiconductors are under increasing consideration for low-cost and large-area applications such as display control circuitry,[1−3] radio frequency transponders,[4] and sensor arrays.[5,6] An attractive feature of these materials is their capability, in some cases, for liquid-phase deposition. Regioregular poly(hexylthiophene) may be cast into films with mobilities of about 0.01 cm^2/Vs, approaching 0.1 cm^2/Vs in exceptional cases.[7] Recently, copolymers with improved stability and on/off ratio have been described by a group at Palo Alto Research Center. The semiconducting phases of these polymers feature extended conjugated segments interacting through pi−pi interactions, enforced by the organization of side chains.

Polycrystalline films of dialkyl oligomers of thiophene and co-oligomers of thiophene and phenylene have also been deposited directly from solution.[8] Recently, a disubstituted pentacene derivative was shown to be sufficiently soluble for deposition.[9] Pentacene itself has been deposited via soluble Diels−Alder adducts.[10] High mobility in oligomeric materials arises from a layered crystal packing motif, with sheets of conjugated rods packed in two dimensions, and end substituents extending in the direction perpendicular to the sheets. While these films are less continuous than polymer films, their compositions are more homogeneous and high on/off ratios for devices handled in air are more routinely obtained. In addition, orbital energy levels and self-assembly properties are easier to control in the oligomers by straightforward changes in ring sequence and end substituents.[11]

Despite the importance of optimizing the quality and uniformity of solution-deposited oligomer films, there is very little understanding of the mechanism by which the films nucleate and grow. It is not known whether the assembly of the semiconductor molecules is initiated in the bulk of the solution or at one of the solution pool interfaces. It has not yet been established whether the initial condensed phase of the semiconducting material is a pure crystal or a lyotropic (solvent-containing) liquid crystal. Most important, it has not been determined whether the connectivity of the grains and the concentration of gross defects in the film, both of which directly limit mobility, arise from the environment or are intrinsic to the film growth mechanism.

In this manuscript, we study the solution deposition of one exemplary semiconductor oligomer, 5,5′-bis(4-hexylphenyl)-2,2′-bithiophene (6PTTP6) from the relatively nontoxic xylene solvent. This compound is synthesized in two simple steps from commercially available 1-bromo-4-hexylbenzene and 2,2′-bithiophene.[8] We have previously reported that both sublimed and solution-cast films of this compound are highly organized into a layered structure, with many orders of diffraction and at least two polymorphs observed by X-ray. The sublimed film has an FET hole mobility of nearly 0.1 cm^2/Vs, while preliminary experiments showed that even the solution-deposited film has a mobility above 0.01 cm^2/Vs and an on/off ratio of 10^4, with all characterizations done in air.[8]

In the present study, the grain structure is compared for films prepared in the open air and in a closed, static atmosphere saturated with xylene vapor. The effect of surface functional groups affixed to the dielectric substrate on the grain appearance and film mobility is probed, to determine optimal fabrication conditions for films with usable mobility, high on/off ratio, and good uniformity. A single crystal device, also obtained from solution deposition under a particular set of conditions, is characterized and displays an expected higher mobility. Mesophases are identified in the presence and absence of the xylene and tentatively identified through polarized optical microscopy (POM). Finally, a preliminary observation of the film evolution using an in situ X-ray diffraction (XRD) technique is reported.

† Part of the special issue "Alvin L. Kwiram Festschrift".

* To whom correspondence should be addressed. E-mail: hek@lucent.com.
‡ Bell Laboratories.
§ Brookhaven National Laboratories.

10.1021/jp037068w CCC: $27.50
Published on Web 02/06/2004

TABLE 1: Electrical Performance of 6PTTP6 Films as a Function of Silane Treatment of the Dielectric Surface

surface type	mobility ($cm^2 V^{-1} s^{-1}$)	on/off ratio
ClPh	2.3×10^{-2}	8×10^3
Ph	2.1×10^{-2}	7×10^3
octadecyltrimethoxy	3.3×10^{-3}	2×10^2
tridecafluoro	2.0×10^{-2}	2×10^4
memo	3.2×10^{-3}	2×10^3
control (no silane)	1.1×10^{-2}	5×10^3

II. Experimental Section

The field-effect measurements were carried out on top-contact FETs, prepared by applying 6PTTP6 in xylenes dropwise onto a substrate maintained at approximately 125 °C. The substrate was a heavily doped silicon wafer, used as a shared gate, with a 300-nm-thick SiO_2 insulating layer, used as the gate dielectric. The solution from which the film grew was contained inside rectangles of 1−2 cm^2 bounded by a fluorinated polymer (3M-722), which was not wetted or dissolved by xylene. Gold source and drain electrodes were evaporated on top of the films through shadow masks, producing channels 4-mm wide and 0.2-mm long. Shorter channel devices were obtained by using a 6-μm-diameter tungsten wire as a mask during gold deposition. The mobility is extracted for the FET biased in the saturation regime with a V_{DS} value of −100 V.

Mesophases were observed on a hot stage using standard techniques of POM and XRD. X-ray reflectivity measurements were carried out at beamline ×22A at the National Synchrotron Light source with a wavelength, $\lambda = 1.16$ Å. Grazing incident angle scattering measurements were carried out at ×22B with a wavelength, $\lambda = 1.55$ Å using a 134-mm MAR X-ray CCD camera. The horizontal sample geometry allowed in-situ investigations of the diffraction pattern during solvent evaporation.

III. Results: Surface Functional Groups and Environmental Effects

Thin layers of silane coupling agents terminated in various functional groups were added to the SiO_2 surface by exposure of a pirhana-cleaned (sulfuric acid:30% hydrogen peroxide 3:1) wafer to the silane as a 1% solution in hot toluene for 5−10 min. These functional silanes included chlorophenylmethyldichloro (ClPh) silane, phenyltriethoxy (Ph) silane, octadecyltrimethoxy silane, tridecafluoro-1,1,2,2-tetrahydrooctyltriethoxy silane, and methacryloxypropyldimethylmethoxy (Memo) silane. For this survey, semiconducting films were grown in the open on a 125° hot plate.

TABLE 2: Comparison of 6PTTP6 Devices Grown under Closed, Equilibrating Conditions and in Open Air

	closed environment		open environment	
surface group	mobility ($cm^2 V^{-1} s^{-1}$)	on/off ratio	mobility ($cm^2 V^{-1} s^{-1}$)	on/off ratio
ClPh	3.9×10^{-2}	10^4	2.3×10^{-2}	10^3
Ph	3.2×10^{-2}	10^4	2.1×10^{-2}	10^3

The promising electrical properties shown in Table 1 for the ClPh silane and Ph silane prompted us to concentrate additional effort toward surfaces with those functional groups. The favorable electrical characteristics imparted by the fluorinated surface were also noteworthy and consistent with a previous observation. However, the fluorinated surface was not pursued further because of the lesser ability to confine a film with a fluoroploymer on this surface.

During solution deposition, the effect of atmospheric turbulence and solvent-vapor equilibration on the molecular packing of the thin films of organic materials in 6PTTP6 was analyzed by growing films under an inverted crystallizing dish where excess xylene was allowed to boil around the film. This "closed environment" was compared to the standard open air method.

On the basis of Table 2, it seems that the reduced atmospheric turbulence produced somewhat higher mobilities and on/off ratios. The highest mobility was observed with the ClPh surface modification in both cases. The films in the closed environment were all deposited at the boiling point of xylenes. The effect of the different conditions on the morphology is especially apparent by optical microscopy. Figure 1 shows images of the film grain structure deposited in a turbulent, or open-air environment: (A)

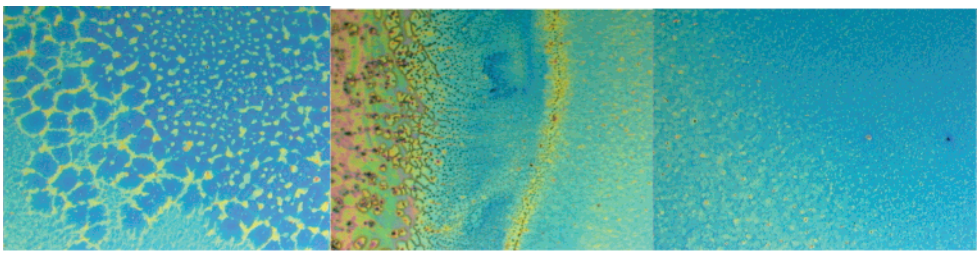

Figure 1.

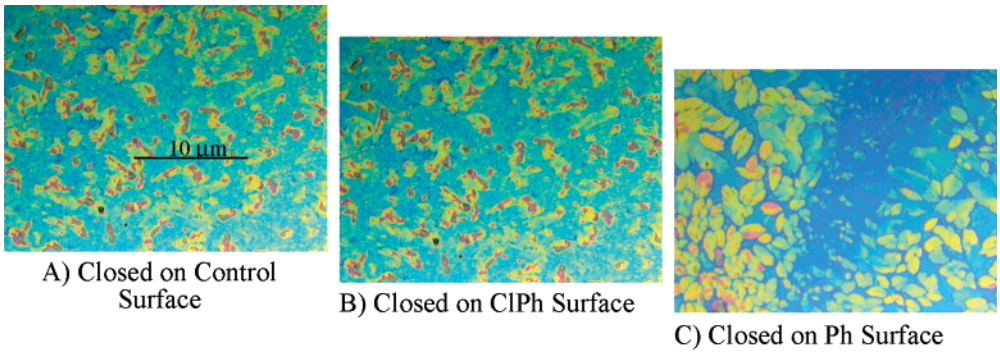

Figure 2.

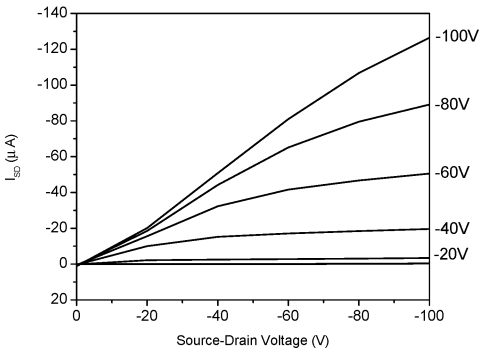

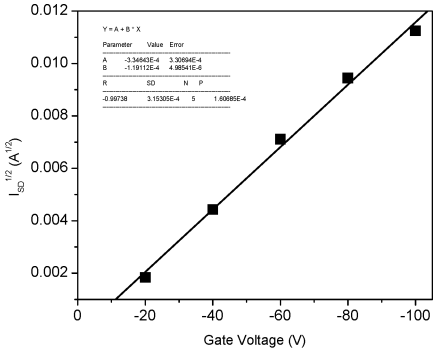

Figure 3.

TABLE 3: Comparison of 6PTTP6 Devices Deposited from Solution at Different Temperatures

temperature (°C)	mobility ($cm^2\ V^{-1}\ s^{-1}$)	on/off ratio
100	7.8×10^{-3}	10^2
115	1.0×10^{-2}	10^3
125	2.4×10^{-2}	10^4
135	1.1×10^{-2}	10^4

no surface modifications; (B) the surface was modified with a monolayer of ClPh silane; and (C) the surface was modified with a monolayer of Ph silane. These three images represent more kinetically controlled structures, since xylene evaporation from the film is completely irreversible.

However, in the presence of a saturated xylene atmosphere, where evaporation from the film is somewhat reversible and atmospheric turbulence is kept to a minimum, the grains are larger and more tightly packed. The images in Figure 2 show grain growth on three different surfaces when deposited in a xylene-saturated, reduced turbulence, "closed" environment: (A) no surface modifications; (B) the surface was modified with a monolayer of ClPh silane; and (C) the surface was modified with a monolayer of Ph silane.

We verified our previous observation that there is an optimal temperature for depositing these films. A set of substrates was placed on a hot plate, aliquots from a common solution were applied to individual substrates in sequence as the temperature rose from 100 °C to 140 °C, and morphology and structure of these films was analyzed. It is shown in Table 3 that substrate temperature has a substantial effect upon the thin film properties. Furthermore, although there may have been uncertainty in the nominal temperature of any particular surface as material was deposited, the temperature differences among surfaces are well established, and the existence of the optimal temperature window is confirmed.

To obtain a useful morphology, the temperature must be elevated during the growth of the solid film. Deposition of grains at ambient temperature does not result in grain interconnection, and a subsequent high-temperature anneal does not improve the morphology. This is consistent with a previous observation, where the dewetting of a softened grain actually results in grain area shrinkage, rather than a spreading of the grains toward each other.[12]

In an extension of this work, device channels were created on a 125° film on oxide using a 6-micron wire and attaching it to the shadow mask before evaporation. The resulting OTFTs have a channel length and width of 8- and 130-μm, respectively, smaller than the size of grains produced under these conditions. The highest mobility exhibited in the saturation regime was 0.15 $cm^2\ V^{-1}\ s^{-1}$ with a good current modulation, or on/off ratio. Figure 3 shows a plot of the measured drain current as a function of source-drain voltage for a range of gate bias voltages. The mobility has very low gate voltage dependence and a threshold voltage around −10 V.

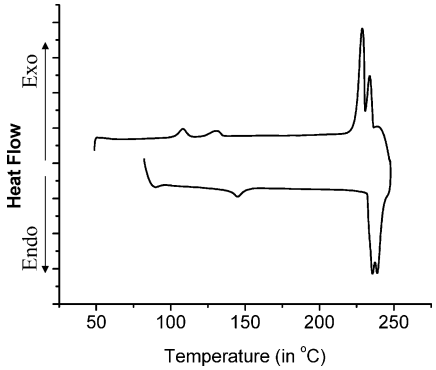

Figure 4. Heating and cooling DSC data for 6PTTP6.

IV. Thermotropic and Lyotropic Mesophases

In our earlier publication, the thermotropic transitions of 6PTTP6 were observed by differential scanning calorimetry (DSC), though not by POM or XRD techniques.[8] From the cooling curve of the DSC data, we can identify four distinct transitions. These are melt-liquid crystal (LC) transition at 233 °C and further crystallization at 228 °C followed by two solid-state LC transitions at 128 °C and 106 °C. For this study, a sample was mounted between glass slides on a hot stage and the various phase changes were monitored by POM. As we cool the sample from its isotropic state at 260 °C, batonnets start appearing from the isotropic melt and develop into a characteristic fanlike smectic A (S_A) texture at 233 °C. As the sample goes through crystallization, the LC phase is frozen into a higher order smectic phase (S_B or S_F). No further changes were observable by POM.

Our main interest in examining these LC phases is to understand the process of film formation as the solvent evaporates. If the film formed by solution evaporation has any LC ordering, it should be possible to view the process by POM in the presence of solvent. We conducted preliminary studies from a 400 ppm solution of 6PTTP6 by placing a few drops on a hot stage at 120 °C and continuously monitoring as the solvent evaporated (Figure 6a). The sample became highly birefringent as the solvent evaporated, consistent with the formation of a layered LC phase. However, crystallization of the sample could occur alongside the LC phase formation, which would be hard to distinguish by POM.

V. X-ray Scattering

In Figure 7, we show X-ray reflectivity (along the surface normal axis) for two samples, one prepared by vacuum

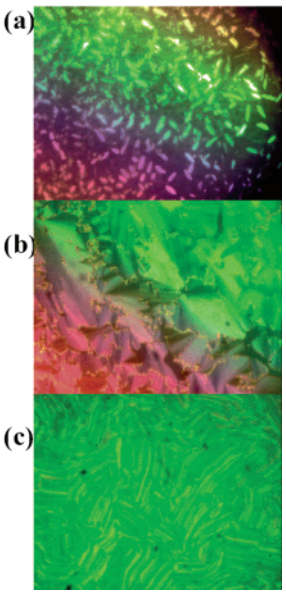

Figure 5. POM micrographs of 6PTTP on cooling from isotropic melt at 260 °C: (a) formation of batonnets from isotropic melt at 240 °C, (b) focal conic texture at 230 °C characteristic of S_A phase, (c) higher order smectic (S_B or S_F) below 200 °C.

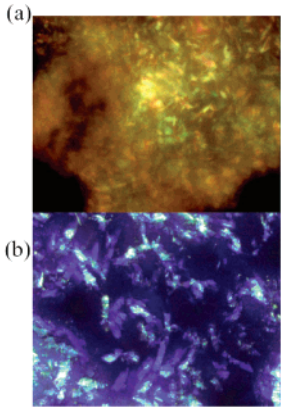

Figure 6. Polarized optical micrographs of 6PTTP solution in xylene as the solvent evaporates from (a) concentrated solution at 120 °C (b) from dilute solution at 120 °C.

deposition and the other prepared by xylene evaporation at 120 °C. Both curves are plotted on the same intensity scale and the intensity has been multiplied by Q_z^2. In the vacuum-deposited sample, at least 10 resolution-limited Bragg peaks are observed and these can be indexed by a single q-vector of 0.207 Å^{-1}. This corresponds to a layer spacing of 30.35 Å. In addition, there are noticeable Kiessig fringes between the first two Bragg peaks and this results from a well-defined film with a thickness of about 15 layers. Further, the rocking scans through these peaks are resolution-limited, with a rocking curve width less than 0.05° fwhm and there is no noticeable mosaic. This corresponds to a lateral correlation length close to 1 μm. Thus, the vaccum-deposited sample exhibits a very well-defined monolayer phase and the layer spacing is close to the molecular length.

Temperature-dependent X-ray studies on melts cooled from the isotropic state confirm the transition from isotropic to S_A to a higher order LC phase at temperatures which correlate with the POM data. However, further analysis of the d spacing is required to identify the higher order smectic phase at lower temperature.

Room-temperature X-ray diffraction data obtained from as-synthesized powders (from solutions) of 6PTTP6, as well as sublimed powders, exhibit polymorphism. Two different d spacings are observed in as-synthesized powders, a minor phase with c* = 29.3 Å and a major phase with c* = 25.3 Å. The sublimed powders, however, display two d spacings of c* = 30.35 Å and c* = 26.4 Å consistent with the vacuum-deposited and the solution-grown films. Clearly, polymorphism is present, with the crystallization path and thermal history strongly influencing the molecular packing of the 6PTTP6 molecules.

For the xylene-deposited sample, we observe polymorphic behavior, as evidenced by the two low-order Bragg peaks, one at 0.207 Å^{-1} and the second at 0.238 Å$^{-1,}$ (positions close to the monolayer spacing), and a third peak at 0.425 Å^{-1}. The latter peak cannot be indexed by either of the first two peaks. All of these peaks are broader than for the vacuum-deposited sample, thus indicating a less ordered structure. The presence of two peaks around 0.22 Å^{-1} suggests the coexistence of two phases, one again with the same 30.35 Å layer spacing as the vacuum-deposited sample, and the second peak with a layer spacing of 26.4 Å, consistent with the powder diffraction. This shorter spacing suggests that the second phase is tilted, with a tilt angle of 29.5°. This is the expected tilt for simple chain molecules (~5 Å diameter) when the neighboring chains are displaced from one another by two carbon atoms. Therefore, it seems plausible that there is a coexistence of at least two phases for the xylene-deposited sample, one phase which is similar to the vacuum-deposited sample and one which is tilted. On the basis of the present measurements, we cannot ascertain the spatial positions of the two phases within the sample, although one of the phases likely has a preference for the substrate interface. Further, the absence of higher order peaks and the peak broadening suggest more disorder in the xylene-deposited samples.

We have also carried out studies of the in-plane structure with grazing incidence diffraction using a CCD camera. The sample was averaged over a range of azimuthal angles so as to create a good powder pattern. Here, the positions of the peaks are given by ($q_{x,y}$, q_z) where $q_{x,y}$ is the in-plane component and q_z is the surface normal component. The four lowest-order diffraction peaks are at (1.295 Å^{-1}, 0.10 Å^{-1}), (1.295 Å^{-1}, 032 Å^{-1}), (1.295 Å^{-1}, 0.55 Å^{-1}), and (1.345 Å^{-1}, 0.68Å^{-1}). The first three peaks all have the value of $q_{x,y}$ and the three peaks are equally spaced along q_z. These peaks can be reasonably well-indexed as the (11), (13), and (15) where c* is half the value of the 0.207 Å^{-1} lattice constant measured from the specular reflectivity, thus suggesting that these peaks correspond to the "untilted" phase of the vacuum-deposited sample. The value of c* suggests that there are two molecules per unit cell which are centered. Assuming that there are no additional low-order peaks associated with this phase, then the phase must be hexagonal in-plane order with a lattice spacing of 5.6 Å and a lateral area of 27.2 Å^2 per molecule. At elevated temperatures, above about 120 °C, these three peaks vanish, leaving only the peak at (1.345 Å^{-1}, 0.65Å^{-1}). This suggests that this peak originates from a different mesophase, perhaps the same phase which contributes the peak at 0.238 Å$^{-1.}$ Finally, the same features could also be observed in samples prepared from xylene in situ. A broad rod of scattering emerges at $q_{x,y}$ = 1.295 Å$^{-1,}$ which evolves into the three collinear spots. The initial broad rod of scattering is indicative of an intermediate lyotropic-like smectic phase which does not have a well-defined stacking sequence.

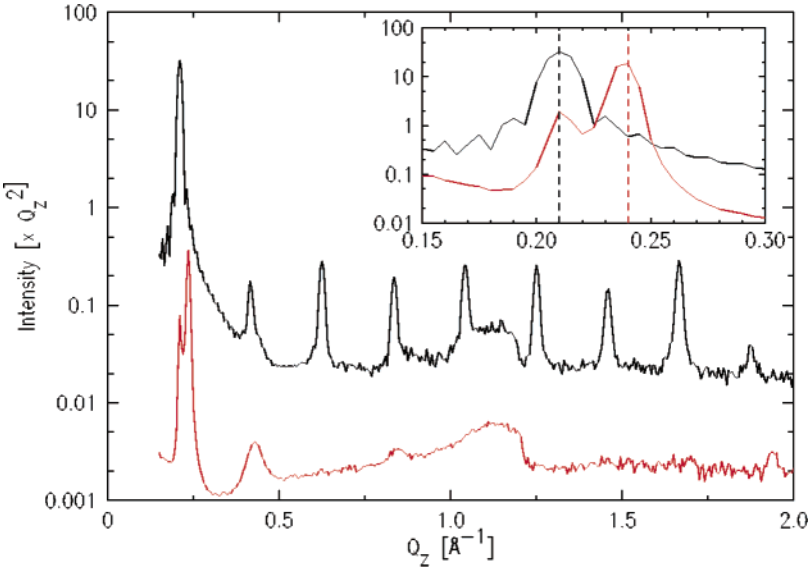

Figure 7. XRD data for sublimed (black, above) and solution-deposited (red) 6PTT6.

VI. Discussion

Experimental results illustrate that 6PTTP6 exhibits a liquid crystalline phase while in solution at 125 °C as seen in the above POM experimental analysis. This phase represents an important intermediate on the path to an oriented and interconnected solid film from solution. Regarding previous attempts to solution-deposit semiconducting films, the lack of moderate temperature liquid crystallinity as a possible stage in the film growth process may explain why so many other organic solids do not form continuous, oriented films from solution. Where liquid crystallinity can be reached, but only at very high temperatures, the mechanical stresses induced on cooling also lead to morphological discontinuity.[12] A further effect of lyotropic liquid crystallinity may be to provide a pathway to polymorphs, as multiple mechanisms for forming the solid film or incomplete conversion from a mesophase to the "crystal" phase can result in a film containing a mixture of packing arrangements. Interestingly, however, this polymorphism does not prevent the formation of domains with single-crystal-like mobility.[13]

With surface modifications, the mobility and on/off ratio can be increased to an average value of 0.03 $cm^2\ V^{-1}\ s^{-1}$ and by 1 order of magnitude from 10^4 to 10^5, respectively. This mobility value for the solution-deposited film approaches that of the vacuum-evaporated film. If we assume that the initial aggregation of 6PTTP6 molecules into at least a lyotropic liquid crystal phase occurs at the *air*−solution interface, then the role of the surface groups is to allow the solution to spread and to prevent the dewetting of lyotropic liquid crystal domains as the last of the solvent is removed. To optimize this process further, solvents and active compounds should both be selected with minimum surface energies. The ones used here are already fairly low, and the phenyl surface modification may contribute additional favorable aromatic interactions at the substrate−solution interface. On the other hand, if the solid film grows at the substrate interface originally, then functionalization of the substrate surface will affect the nucleation of the solid or the spreading of the solid (possible in its lyotropic form) into a flat, macroscopic domain favorable for high semiconductor mobility.

The ultimate mobility from an oligomeric semiconductor would be obtained from a device with no grain boundaries. For solution depositing of the oligomeric semiconductor, the single-crystal-like mobilities we obtained here are the highest mobilities reported to date. The procedures and mechanisms uncovered here may lead to a more generally applicable route to all-printed organic transistors with mobilities >0.1 cm^2/Vs as well as improved stability.[14]

References and Notes

(1) Blanchet, G. B.; Loo, Y. L.; Rogers, J. A.; Gao, F.; Fincher, C. R. *Appl. Phys. Lett.* **2003**, *82*, 463−465.

(2) Rogers, J.; Bao, Z.; Baldwin, K.; Dodabalapur, A.; Crone, B.; Raju, V. R.; Katz, H. E.; Kuck, V.; Amundson, K.; Jay Ewing, J.; Drziac, P. *Proc. Natl. Acad. Sci.* **2001**, *98*, 4835−4840.

(3) Huitema, H. E. A.; Gelinck, G. H.; van der Putten, J.; Kuijk, K. E.; Hart, K. M.; Cantatore, E.; de Leeuw, D. M. *Adv. Mater.* **2002**, *14*, 1201.

(4) Baude, P. F.; Ender, D. A.; Haase, M. A.; Kelley, T. W.; Muyres, D. V.; Theiss, S. D. *Appl. Phys. Lett.* **2003**, *82*, 3964−3966.

(5) Crone, B.; Dodabalapur, A.; Gelperin, A.; Torsi, L.; Katz, H. E.; Lovinger, A. J. *Appl. Phys. Lett.* **2001**, *78*, 2229.

(6) Zhu, Z. T.; Mason, J. T.; Dieckmann, R.; Malliaras, G. G. *Appl. Phys. Lett.* **2002**, *81*, 4643−4645.

(7) Sirringhaus, H.; Tessler, N.; Friend, R. H. *Science* **1998**, *280*, 1741−1744.

(8) Mushrush, M.; Facchetti, A.; Lefenfeld, M.; Katz, H. E.; Marks, T. J. *J. Am. Chem. Soc.* **2003**, *125*, 9414−9423.

(9) Anthony, J. E.; Eaton, D. L.; Parkin, S. R. *Organic Lett.* **2002**, *4*, 15−18.

(10) Afzali, A.; Dimitrakopoulos, C. D.; Breen, T. L. *J. Am. Chem. Soc.* **2002**, *124*, 8812−8813.

(11) Hong, X. M.; Katz, H. E.; Lovinger, A. J.; Wang, B.-C.; Raghavachari, K. *Chem. Mater.* **2001**, *13*, 4686−4691.

(12) Torsi, L.; Dodabalapur, A.; Lovinger, A. J.; Katz, H. E.; Ruel, R.; Davis, D. D.; Baldwin, K. W. *Chem. Mater.* **1995**, *7*, 2247−2251.

(13) Podzorov, V.; Pudalov, V. M.; Gershenson, M. E. *Appl. Phys. Lett.* **2003**, *82*, 1739−1741.

(14) Someya, T.; Katz, H. E.; Gelperin, A.; Lovinger, A. J.; Dodabalapur, A. *Appl. Phys. Lett.* **2002**, *81*, 3079−3081.